

Study of energy transfer in gadolinium – gallium garnet crystals doped with Yb³⁺ and Ho³⁺ ions

A.M. Belovolov, M.I. Belovolov, E.M. Dianov,
M.A. Ivanov, V.V. Kochurikhin, V.V. Randoshkin

Abstract. The luminescence kinetics of Yb³⁺ donors and Ho³⁺ acceptors is quantitatively studied in gallium–gadolinium garnet (GGG) crystals doped with Yb³⁺ and Ho³⁺ ions. It is shown that the sensitisation of transitions in Ho³⁺ ions occurs due to migration-accelerated (hopping) energy transfer. The microparameters of donor–donor energy transfer are determined at 300 and 77 K. The microparameters of donor–acceptor energy transfer are found at the same temperatures at the first stage of successive sensitisation (resulting in the population of the ⁵I₆ state of Ho³⁺ ions) and at the second stage of successive sensitisation of the ⁵S₂, ⁵F₄ → ⁵I₈ transition in Ho³⁺ ions. At the second stage of sensitisation, the values of the microparameter of reverse energy transfer are also determined. The possibility of obtaining lasing at sensitised transitions in Ho³⁺ ions in Yb³⁺:Ho³⁺:GGG crystals pumped into the absorption band of Yb³⁺ ions is discussed.

Keywords: energy transfer, sensitisation of transitions, luminescence kinetics, energy transfer microparameters.

1. Introduction

Interest in active media co-doped with the Yb³⁺ (donors) and Ho³⁺ (acceptor) ions is caused by many transitions in Ho³⁺ ions which can be efficiently sensitised to obtain lasing [1–6]. At present laser action was obtained at the 1.208-μm ⁵I₆ → ⁵I₈ [1], 2.9-μm ⁵I₆ → ⁵I₇ [1, 3], 2.2-μm ⁵I₇ → ⁵I₈ [3, 4], and 0.54-μm ⁵S₂, ⁵F₄ → ⁵I₈ [5, 6] transitions of Ho³⁺ ions sensitised due to energy transfer. The latter transition is sensitised due to multistage (successive) energy transfer, and lasing at this transition was obtained only at 77 K (probably because of the thermal activation of reverse energy transfer at the second stage of sensitisation).

As a rule, the sensitisation of Ho³⁺ ions has been studied only qualitatively or semi-qualitatively in the best case [3–8, 11]. Although the basic energy transfer and relaxa-

tion processes in systems co-doped with the Yb³⁺ and Ho³⁺ ions were identified in these studies, no quantitative analysis was performed. The difficulties of the theoretical description of energy transfer in the Yb³⁺ – Ho³⁺ system are explained by the following reasons:

(i) migration-accelerated Yb³⁺ → Ho³⁺ energy transfer [7–9];

(ii) the presence of the long-lived ⁵I₇ level (with the lifetime ~ 10 ms) of the Ho³⁺ ion, so that the energy relaxation on the acceptor cannot be considered rapid;

(iii) reversible energy transfer at the second stage of sensitisation of the ⁵S₂, ⁵F₄ → ⁵I₈ transition in Ho³⁺ ions [8, 10].

In the case of migration-accelerated energy transfer, a spherical spatial region exists inside which the probability of donor excitation quenching by an acceptor exceeds the probability of the escape of donor excitation from an acceptor under consideration due to migration (i.e. donor–donor energy transfer). This spatial region was called a strong-quenching sphere or ‘black sphere’ because within the framework of simplest models the donor excitation entering into it is completely quenched by the acceptor [12–15]. The physical picture of migration-accelerated energy transfer depends on the relation between the black-sphere radius R_w and the characteristic length λ of a migration hop which is usually assumed equal to the mean distance between donors [12–15]. When the inequality $R_w \ll \lambda$ is fulfilled, the hopping mechanism of migration-accelerated energy transfer takes place, which is characterised by so small strong-quenching sphere that donor excitation cannot perform hops inside the black sphere, and one hop is enough for excitation to leave the sphere.

Theoretical studies of the hopping regime performed in [12–14] were based on different models of hopping quenching. The approaches developed in these papers were used to calculate the luminescence kinetics of donors after their excitation by a short optical pulse. It was assumed in models [12–14] that the excitation level of donors was low, the donor–acceptor energy transfer is irreversible, and the relaxation of energy in acceptors is instant. Therefore, models [12–14] can be applied only to interpret the luminescence kinetics of donors upon weak excitation of the donor subsystem and cannot be in principle used for studying the successive sensitisation of high energy levels of the acceptor. Note that the luminescence kinetics of the Yb³⁺ ions in phosphate glasses doped with Yb³⁺ and Ho³⁺ ions was studied in [9] by using models [12–14]. It was found in [9] that in the case of weak excitation of the donor subsystem, the hopping mechanism of sensitisation of Ho³⁺

A.M. Belovolov, M.I. Belovolov, E.M. Dianov Fiber Optics Research Center, Russian Academy of Sciences, ul. Vavilova 38, 119991 Moscow, Russia; e-mail: bmi@fo.gpi.ru;

M.A. Ivanov, V.V. Kochurikhin, V.V. Randoshkin A.M. Prokhorov General Physics Institute, Russian Academy of Sciences, ul. Vavilova 38, 119991 Moscow, Russia

Received 12 April 2006; revision received 25 May 2006

Kvantovaya Elektronika 36 (8) 702–712 (2006)

Translated by M.N. Sapozhnikov

ions takes place; also, the microparameters of donor–donor and donor–acceptor energy transfer were measured.

In [2], the model of hopping step sensitisation of luminescence of Ho^{3+} ions in solids doped with Yb^{3+} and Ho^{3+} ions was developed. This model takes into account both the finite lifetimes of acceptor levels and reversible energy transfer at the second sensitisation stage of the ${}^5\text{S}_2, {}^5\text{F}_4 \rightarrow {}^5\text{I}_8$ transition in Ho^{3+} ions. This makes it possible to calculate the luminescence kinetics for donors and acceptors.

The aim of our paper is to study experimentally the luminescence kinetics of donors and acceptors in $\text{Yb}^{3+} : \text{Ho}^{3+}$ GGG crystals and to analyse quantitatively these kinetics based on the model of hopping step sensitisation developed in [2].

2. Hopping model of sensitisation of Ho^{3+} ions in solids activated by Yb^{3+} and Ho^{3+} ions (theory)

The model of hopping sensitisation of Ho^{3+} ions in solids activated by Yb^{3+} and Ho^{3+} takes into account the following main channels of energy transfer and relaxation which were found in papers [1, 3–7, 10, 11] (Fig. 1):

(1) The channel of linear sensitisation of luminescence of Ho^{3+} ions including the following processes:

(i) irreversible energy transfer from the excited Yb^{3+} ion to the unexcited Ho^{3+} ion accompanied by the transition of the latter to the ${}^5\text{I}_6$ state;

(ii) the radiative relaxation of Ho^{3+} ions from the ${}^5\text{I}_6$ state to the ${}^5\text{I}_8$ state (the luminescence wavelength is $\sim 1.2 \mu\text{m}$) and relaxation of the Ho^{3+} ion from the ${}^5\text{I}_6$ state to the metastable ${}^5\text{I}_7$ state;

(iii) radiation at the ${}^5\text{I}_7 \rightarrow {}^5\text{I}_8$ transition of Ho^{3+} ions (the luminescence wavelength is $\sim 2.1 \mu\text{m}$).

(2) The channel of successive sensitisation of anti-Stokes luminescence at the ${}^5\text{S}_2, {}^5\text{F}_4 \rightarrow {}^5\text{I}_8$ and ${}^5\text{S}_2, {}^5\text{F}_4 \rightarrow {}^5\text{I}_7$ transitions of Ho^{3+} ions (the luminescence wavelengths are $\sim 535 - 560 \text{ nm}$ and $\sim 740 - 770 \text{ nm}$, respectively) including the following processes:

(i) irreversible energy transfer from the excited Yb^{3+} ion to the unexcited Ho^{3+} ion accompanied by the transition of the latter to the ${}^5\text{I}_6$ state (the first stage of successive sensitisation);

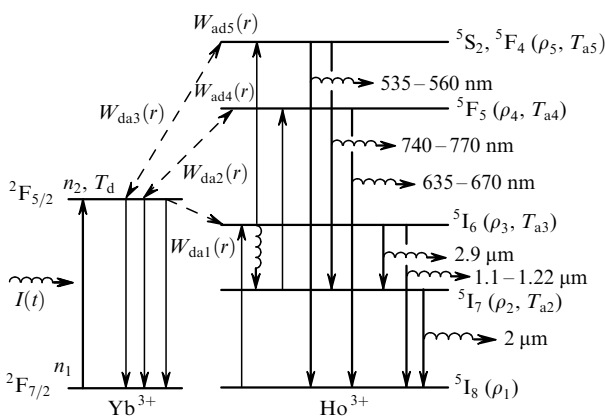


Figure 1. Processes of energy transfer and relaxation considered in the model of hopping sensitisation of Ho^{3+} ions in solids doped with Yb^{3+} and Ho^{3+} ions [1, 3–7, 10, 11].

(ii) reversible (in the general case) energy transfer from the excited Yb^{3+} ion to the unexcited Ho^{3+} ion in the ${}^5\text{I}_6$ state accompanied by the transition of the latter to the ${}^5\text{S}_2, {}^5\text{F}_4$ state (the second stage of successive sensitisation);

(iii) the radiative relaxation of Ho^{3+} ions at the ${}^5\text{S}_2, {}^5\text{F}_4 \rightarrow {}^5\text{I}_8$ и ${}^5\text{S}_2, {}^5\text{F}_4 \rightarrow {}^5\text{I}_7$ transitions.

(3) The channel of nonlinear quenching of the ${}^5\text{I}_7$ state of Ho^{3+} including the following processes:

(i) reversible (in the general case) energy transfer from the excited Yb^{3+} ion to the excited Ho^{3+} ion in the ${}^5\text{I}_7$ state accompanied by the transition of the latter to the ${}^5\text{F}_5$ state;

(ii) the radiative relaxation of Ho^{3+} ions at the ${}^5\text{F}_5 \rightarrow {}^5\text{I}_8$ transition;

(iii) the nonradiative relaxation of Ho^{3+} at the ${}^5\text{F}_5 \rightarrow {}^5\text{I}_6$ transition.

The system of kinetic equations for populations of the states of Yb^{3+} and Ho^{3+} ions in the hopping migration mechanism written for the case of an activated crystal lattice has the form [2]

$$\frac{\partial f(r_k, t)}{\partial t} = - \left[\sum_{i=1}^3 W_{\text{dai}}(r_k) \rho_i(t) \right] f(r_k, t) + \sigma_d \frac{I(t)}{h\nu} \frac{1-f(r_k, t)}{n_2(t)} + \sum_{i=4}^5 \frac{\rho_i(t)}{n_2(t)} W_{\text{adi}}(r_k) + \frac{1-f(r_k, t)}{\tau_0}, \quad (1)$$

$$\frac{dn_2(t)}{dt} = - \frac{n_2(t)}{T_d} - yn_2(t) \times \left[\sum_{i=1}^3 \rho_i(t) \sum_k W_{\text{dai}}(r_k) f(r_k, t) \right] + \sigma_d \frac{I(t)}{h\nu} [1 - 2n_2(t)] + y \left\{ \sum_{i=4}^5 \rho_i(t) \sum_k W_{\text{adi}}(r_k) [1 - n_2(t) f(r_k, t)] \right\}, \quad (2)$$

$$n_1(t) = 1 - n_2(t), \quad (3)$$

$$\frac{d\rho_2(t)}{dt} = - \frac{\rho_2(t)}{T_{a2}} + \sum_{i=3}^5 W_{i2} \rho_i(t) - x\rho_2(t)n_2(t) \times \sum_k W_{\text{da2}}(r_k) f(r_k, t) + x\rho_4(t) \sum_k W_{\text{ad4}}(r_k) \times [1 - n_2(t) f(r_k, t)], \quad (4)$$

$$\frac{d\rho_3(t)}{dt} = - \frac{\rho_3(t)}{T_{a3}} + \sum_{i=4}^5 W_{i3} \rho_i(t) + x\rho_1(t)n_2(t) \times \sum_k W_{\text{da1}}(r_k) f(r_k, t) - x\rho_3(t)n_2(t) \sum_k W_{\text{da3}}(r_k) f(r_k, t) + x\rho_5(t) \sum_k W_{\text{ad5}}(r_k) [1 - n_2(t) f(r_k, t)], \quad (5)$$

$$\frac{d\rho_4(t)}{dt} = - \frac{\rho_4(t)}{T_{a4}} + x\rho_2(t)n_2(t) \sum_k W_{\text{da2}}(r_k) f(r_k, t) - x\rho_4(t) \sum_k W_{\text{ad4}}(r_k) [1 - n_2(t) f(r_k, t)], \quad (6)$$

$$\frac{d\rho_5(t)}{dt} = -\frac{\rho_5(t)}{T_{a5}} + x\rho_3(t)n_2(t) \sum_k W_{da3}(r_k)f(r_k, t) - x\rho_5(t) \sum_k W_{ad5}(r_k)[1 - n_2(t)f(r_k, t)], \quad (7)$$

$$\rho_1(t) = 1 - \sum_{i=2}^5 \rho_i(t). \quad (8)$$

Here, $n_j(t)$ ($j = 1, 2$) is the population of the j th state of donors averaged over distances in a donor–acceptor pair; $\rho_i(t)$ ($i = 1 - 5$) is the population of the i th state of the acceptor averaged over distances in a donor–acceptor pair; $f(r_k, t)$ is the probability of finding the excited donor at the instant t at the distance r_k from the acceptor under the condition that at the instant $t = 0$ this donor was excited; T_d is the intracentre excited-state lifetime of donors;

$$T_{a2} = W_{21}^{-1}, \quad T_{a3} = (W_{31} + W_{32})^{-1}, \quad (9)$$

$$T_{a4} = \left(\sum_{i=1}^3 W_{4i} \right)^{-1}, \quad T_{a5} = \left(\sum_{i=1}^4 W_{5i} \right)^{-1}$$

is the intracentre lifetime of the i th excited state of acceptors ($i = 2 - 5$); W_{ik} is the rate of intracentre relaxation from the i th level of the acceptor to its k th level taking into account both radiative and nonradiative transitions; σ_d is the absorption cross section for radiation at frequency ν at the donor transition; $I(t)$ is the intensity of exciting radiation at frequency ν ; $W_{da i}(r)$ is the dependence of the rate of energy transfer from the excited donor to the acceptor in the i th quantum state on the distance r between them; $W_{ad i}(r)$ is the dependence of the rate of inverse energy transfer from the i th excited state of the acceptor to the unexcited donor on the distance r between them; x and y are the concentrations of donors and acceptors, respectively, normalised as

$$x = \frac{N_d}{N_v}, \quad y = \frac{N_a}{N_v}; \quad (10)$$

N_d and N_a are the concentrations of donors (Yb^{3+}) and acceptors (Ho^{3+}), respectively; N_v is the concentration of vacancies accessible for donors and acceptors in the given lattice; and τ_0 is the average time between excitation hops from donor to donor.

The summation over k in (1)–(7) is performed over all the sites of the crystal lattice accessible for activators. The system of equations (1)–(8) was obtained by averaging kinetic equations for a donor–acceptor pair over the distribution of distances between them [2]. Equations (1)–(8) were derived assuming that the inequality

$$\frac{4}{3}\pi R_w^3 N_a \ll 1 \quad (11)$$

is valid where R_w is the radius of a black sphere determined by the equation [12]

$$W_{da1}(R_w) = \tau_0^{-1}. \quad (12)$$

The system of equations for a disordered (continuous) medium is obtained from system (1)–(8) by using the formal substitution

$$y \sum_k \dots \rightarrow 4\pi N_a \int_{r_{\min}}^{\infty} \dots r^2 dr, \quad (13)$$

$$x \sum_k \dots \rightarrow 4\pi N_d \int_{r_{\min}}^{\infty} \dots r^2 dr, \quad f(r_k, t) \rightarrow f(r, t),$$

where integration is performed over the entire volume of the activated medium, and r_{\min} is the minimal possible distance between donors and acceptors in this medium.

We will solve system (1)–(8) for the case of excitation of donors by a short optical pulse of the form $I(t) = E_0 \delta(t)$, where $\delta(t)$ is the Dirac delta function and E_0 is the optical pulse energy. We will seek the solution of system (1)–(8) by the method of successive approximations.

As the first approximation we consider the approximation of weakly excited activators, which is specified by the inequalities

$$n_0 \ll 1, \quad n_0 N_d \ll N_a, \quad (14)$$

where $n_0 = n_2(0)$ is the population of donors immediately after the end of the exciting pulse.

When inequalities (14) are fulfilled, the relations

$$n_2(t) \ll n_1(t), \quad (15)$$

where $n_1(t) \approx 1$, and

$$\rho_i(t) \ll \rho_1(t), \quad (16)$$

where $\rho_1(t) \approx 1$, $i = 2 - 5$, are valid at any moment.

When conditions (15) and (16) are fulfilled, we can omit in Eqns (1), (2), (4), and (5) the terms that are proportional to $\rho_i(t)$, where $i = 2 - 5$, by retaining them only in Eqns (6) and (7).

In the limit of weakly excited activators, the solution of system (1)–(8) with the initial conditions

$$f(r_k, 0) = 1, \quad n_2(0) = n_0, \quad \rho_i(0) = 0 \quad (i = 2 - 5) \quad (17)$$

has the form

$$n_2^{(1)}(t) = n_0 \exp \left[-\frac{t}{T_d} - \int_0^t F_1^{(1)}(\tau) d\tau \right], \quad (18)$$

$$\rho_3^{(1)}(t) = \frac{N_d}{N_a} \int_0^t F_1^{(1)}(\tau) n_2^{(1)}(\tau) \exp \left(\frac{\tau - t}{T_{a3}} \right) d\tau, \quad (19)$$

$$\rho_2^{(1)}(t) = W_{32} \int_0^t \rho_3^{(1)}(\tau) \exp \left(\frac{\tau - t}{T_{a2}} \right) d\tau, \quad (20)$$

$$\rho_4^{(1)}(t) = \frac{N_d}{N_a} \int_0^t F_2^{(1)}(\tau) n_2^{(1)}(\tau) \rho_2^{(1)}(\tau) \exp \left(\frac{\tau - t}{T_{a4}} \right) d\tau, \quad (21)$$

$$\rho_5^{(1)}(t) = \frac{N_d}{N_a} \int_0^t F_3^{(1)}(\tau) n_2^{(1)}(\tau) \rho_3^{(1)}(\tau) \exp \left(\frac{\tau - t}{T_{a5}} \right) d\tau, \quad (22)$$

where

$$\bar{T}_{a4}^{-1} = T_{a4}^{-1} + \bar{W}_{ad4}, \quad \bar{T}_{a5}^{-1} = T_{a5}^{-1} + \bar{W}_{ad5}; \quad (23)$$

$$\bar{W}_{ad4} = x \sum_k W_{ad4}(r_k), \quad \bar{W}_{ad5} = x \sum_k W_{ad5}(r_k); \quad (24)$$

$$F_1^{(1)}(t) = y \sum_k W_{da1}(r_k) f^{(1)}(r_k, t); \quad (25)$$

$$F_2^{(1)}(t) = y \sum_k W_{da2}(r_k) f^{(1)}(r_k, t); \quad (26)$$

$$F_3^{(1)}(t) = y \sum_k W_{da3}(r_k) f^{(1)}(r_k, t); \quad (27)$$

$$f^{(1)}(r_k, t) = \frac{\tau_0 - 1}{W_{da1}(r_k) + \tau_0^{-1}} + \frac{W_{da1}(r_k)}{W_{da1}(r_k) + \tau_0^{-1}} \times \exp\left\{-[W_{da1}(r_k) + \tau_0^{-1}]t\right\}. \quad (28)$$

\bar{W}_{adi} in (23) are the average rates of inverse energy transfer from the i th level of the acceptor to the unexcited donor. The superscript at variables $n_2^{(1)}(t)$, $f^{(1)}(r, t)$ and $\rho_i^{(1)}(t)$ in (18)–(33) denote the first approximation (approximation of weakly excited activators). In the case of multipole interaction mechanism, the rates of energy transfer are

$$W_{dai}(r) = \frac{C_{dai}}{r^m} \quad (i = 1 - 3), \quad W_{adj}(r) = \frac{C_{adj}}{r^m} \quad (j = 4, 5),$$

$$W_{dd}(r) = \frac{C_{dd}}{r^s}, \quad (29)$$

where C_{dai} and m are the microparameter and multipolarity of donor–acceptor energy transfer to the acceptor in the i th state, respectively; C_{adj} is the microparameter of inverse (acceptor–donor) energy transfer from the acceptor in the j th state; C_{dd} and s are the microparameter and multipolarity of the donor–acceptor interaction. Then, we obtain from (18), (25), and (28) that the luminescence kinetics for donors in a crystal lattice has the form [2]

$$n_2^{(1)}(t) = n_0 \exp\left\{-\frac{t}{\bar{T}_d} - y \sum_k \left[\left(\frac{C_{da1}/r_k^m}{C_{da1}/r_k^m + \tau_0^{-1}}\right)^2 \times [1 - \exp[-(C_{da1}/r_k^m + \tau_0^{-1})t]]\right]\right\}, \quad (30)$$

where

$$\bar{T}_d^{-1} = T_d^{-1} + \bar{W}_1; \quad (31)$$

$$\bar{W}_1 = y \sum_k \frac{C_{da1}/r_k^m}{1 + C_{da1}\tau_0/r_k^m}; \quad (32)$$

$$\tau_0 = \int_0^\infty \exp\left\{-\frac{x}{2} \sum_k \left[1 - \exp\left(-\frac{2C_{dd}t}{r_k^s}\right)\right]\right\} dt; \quad (33)$$

\bar{W}_1 is the stationary rate of hopping quenching of donor luminescence; \bar{T}_d is the decay time constant of donor luminescence at the stationary decay stage. The mean time

between excitation hops from donor to donor (33) was determined as in [12] taking into account the reversible nature of donor–donor energy transfer. The luminescence kinetics of donors in a continuous medium is identical to kinetics considered in [13, 14] and, therefore, is not presented here.

Kinetics (30) obtained for the activated crystal lattice has the same qualitative features as the hopping kinetics of donors obtained in papers [12–14] for a continuous medium. Thus, for $t \ll r_{\min}^m/C_{da1}$, excited donors located at the minimal possible distance from acceptors for the given lattice decay exponentially (the stage of statistically ordered decay).

For $r_{\min}^m/C_{da1} < t < \tau_0$, the kinetics of donors (30) becomes nonexponential due to the successive decay of donor excitations inside black spheres at different distances from the acceptor (the stage of disordered decay). For $2\tau_0 < t$, the kinetics of donors (30) becomes exponential because donor excitations initially located outside black spheres decay at this stage (the stationary stage of hopping decay). These donor excitations decay due to entering black spheres during migration. It follows from (30)–(33) that the parameters C_{dd} and s of donor–donor energy transfer and parameters C_{da1} and m of donor–acceptor energy transfer at the first stage of successive sensitisation can be determined from the luminescence kinetics of donors. This can be done by different methods. For example, C_{da1} , m , and τ_0 can be determined by approximating the entire experimental kinetics by dependence (30). This method for determining C_{da1} , m , and τ_0 will be correct if the approximated kinetics has a distinct static decay region. By determining τ_0 for two samples with different concentrations of donors, we can calculate C_{dd} and s by numerical methods from the system of two equations of type (33).

Taking (11) into account in (19)–(22), and (30), we can obtain simple approximate expressions for the luminescence kinetics of donors and acceptors [2]:

$$n_2^{(1)}(t) \approx n_0 \exp\left(-\frac{t}{\bar{T}_d}\right), \quad (34)$$

$$\rho_3^{(1)}(t) = \frac{\bar{W}_1 n_0}{T_{a3}^{-1} - \bar{T}_d^{-1}} \frac{N_d}{N_a} \left[\exp\left(-\frac{t}{\bar{T}_d}\right) - \exp\left(-\frac{t}{T_{a3}}\right) \right], \quad (35)$$

$$\rho_2^{(1)}(t) = \frac{\bar{W}_1 W_{32} n_0}{T_{a3}^{-1} - \bar{T}_d^{-1}} \frac{N_d}{N_a} \left[\frac{(T_{a3}^{-1} - \bar{T}_d^{-1}) \exp(-t/T_{a2})}{(\bar{T}_d^{-1} - T_{a2}^{-1})(T_{a3}^{-1} - T_{a2}^{-1})} - \frac{\exp(-t/\bar{T}_d) + \exp(-t/T_{a3})}{\bar{T}_d^{-1} - T_{a2}^{-1} + T_{a3}^{-1} - T_{a2}^{-1}} \right], \quad (36)$$

$$\rho_4^{(1)}(t) = \frac{\bar{W}_1 \bar{W}_2 W_{32} \bar{T}_{a4} n_0^2}{T_{a3}^{-1} - \bar{T}_d^{-1}} \left(\frac{N_d}{N_a}\right)^2 \times \left[\frac{(T_{a3}^{-1} - \bar{T}_d^{-1}) \exp(-t/T_{a2})}{(\bar{T}_d^{-1} - T_{a2}^{-1})(T_{a3}^{-1} - T_{a2}^{-1})} - \frac{\exp(-t/\bar{T}_d)}{\bar{T}_d^{-1} - T_{a2}^{-1}} + \frac{\exp(-t/T_{a3})}{T_{a3}^{-1} - T_{a2}^{-1}} \right] \exp\left(-\frac{t}{\bar{T}_d}\right), \quad (37)$$

$$\rho_5^{(1)}(t) = \frac{\bar{W}_1 \bar{W}_3 \bar{T}_{a5} n_0^2}{T_{a3}^{-1} - \bar{T}_d^{-1}} \left(\frac{N_d}{N_a}\right)^2 \times$$

$$\times \left[\exp\left(-\frac{2t}{\bar{T}_d}\right) - \exp\left[-(T_{a3}^{-1} + \bar{T}_d^{-1})t\right] \right], \quad (38)$$

where

$$\bar{W}_2 = y \sum_k \frac{W_{da2}(r_k)}{1 + W_{da1}(r_k)\tau_0}, \quad (39)$$

$$\bar{W}_3 = y \sum_k \frac{W_{da3}(r_k)}{1 + W_{da1}(r_k)\tau_0} \quad (40)$$

are the stationary rates of donor–acceptor energy transfer to acceptors in the states 2 and 3, respectively, in the case of a crystal lattice.

Expressions (37) and (38) were derived taking into account that the lifetimes of acceptor levels 4 and 5 (the 5S_2 , 5F_4 , and 5F_5 levels of Ho^{3+} ions) are small [2], which allows one to use the quasi-stationary approximation for determining the populations of these levels.

One can see from (37) and (38) that the stationary rates of energy transfer \bar{W}_2 and \bar{W}_3 characterising the second state of successive sensitisation appear only in the amplitudes of given kinetics. This means that \bar{W}_2 and \bar{W}_3 (and, therefore, microparameters C_{da2} and C_{da3}) cannot be determined from kinetics (37) and (38). The values of \bar{W}_2 and \bar{W}_3 can be estimated from (37) and (38) and measurements of the quantum yield of sensitised luminescence of acceptors at the 5S_2 , ${}^5F_4 \rightarrow {}^5I_8$ and ${}^5F_5 \rightarrow {}^5I_8$ transitions; however, this experimental method is quite complicated and is not accurate enough. Thus, it is reasonable to use the time dependence in expressions (35)–(38) for the experimental verification of the validity of the proposed model of sensitisation processes in the $\text{Yb}^{3+} - \text{Ho}^{3+}$ activator system.

In the second approximation of the model, we will take into account the possibility of accumulation of acceptors in the long-lived 5I_6 and 5I_7 states as a small perturbation, and also the influence of successive sensitisation, proceeding via these states, on the quenching of donors. For this purpose, we consider in (1)–(8) the terms depending on $\rho_i(t)$ ($i = 2 - 5$), which were omitted in the first approximation, by substituting $\rho_i^{(1)}(t)$ into them. In addition, to take into account the possible accumulation of acceptors in the long-lived 5I_6 and 5I_7 states, we set $\rho_1^{(1)}(t) \approx 1 - \rho_2^{(1)}(t) - \rho_3^{(1)}(t)$. Equation (1) can be transformed to obtain (with an accuracy to the second-order terms $[\rho_i^{(1)}(t)]^2$)

$$\begin{aligned} \frac{dn_2^{(2)}(t)}{dt} = & -\frac{n_2^{(2)}(t)}{T_d} - yn_2^{(2)}(t) \sum_k W_{da1}(r_k) f^{(1)}(r_k, t) \\ & - yn_2^{(2)}(t) \sum_{i=2}^3 \rho_i^{(1)}(t) \sum_k [W_{dai}(r_k) \\ & \times (1 - \bar{W}_{ad(i+2)} \bar{T}_{a(i+2)}) - W_{da1}(r_k)] f^{(1)}(r_k, t). \end{aligned} \quad (41)$$

Its solution can be written in the form

$$n_2^{(2)}(t) = n_0 \exp\left[-\frac{t}{T_d} - \int_0^t F_1^{(1)}(\tau) d\tau - \theta(t)\right], \quad (42)$$

where

$$\begin{aligned} \theta(t) = & \bar{W}_1 W_{32} \frac{N_d}{N_a} (\bar{W}_2' - \bar{W}_1) \bar{T}_d T_{a3} n_0 t + \frac{\bar{W}_1 n_0}{T_{a3}^{-1} - \bar{T}_d^{-1}} \frac{N_d}{N_a} \\ & \times [\bar{T}_d (\bar{W}_3' - \bar{W}_1) - \bar{T}_d^2 (\bar{W}_2' - \bar{W}_1) W_{32}] \\ & \times \left[1 - \exp\left(-\frac{t}{\bar{T}_d}\right) \right] - \frac{\bar{W}_1 n_0}{T_{a3}^{-1} - \bar{T}_d^{-1}} \frac{N_d}{N_a} [T_{a3} (\bar{W}_3' - \bar{W}_1) \\ & - T_{a3}^2 (\bar{W}_2' - \bar{W}_1) W_{32}] \left[1 - \exp\left(-\frac{t}{T_{a3}}\right) \right]; \end{aligned} \quad (43)$$

$$\bar{W}_2' = \frac{\bar{W}_2}{1 + \bar{W}_{ad4} T_{a4}}; \quad \bar{W}_3' = \frac{\bar{W}_3}{1 + \bar{W}_{ad5} T_{a5}}. \quad (44)$$

\bar{W}_i' ($i = 2, 3$) in (43) are effective rates of energy transfer at the second stage of successive sensitisation of levels 4 and 5 of Ho^{3+} ions, i.e. the rates of energy transfer determined taking into account the reversible nature of this process. It follows from (44) that the effective rate of energy transfer at the second stage of successive sensitisation drastically decreases if the average rate of inverse energy transfer exceeds the rate of the intracentre decay of levels 4 and 5 of Ho^{3+} ions.

Expression (43) was derived taking into account the relation between the lifetimes of the donor and acceptor states $T_{a2} \gg \bar{T}_d$, T_{a3} in the $\text{Yb}^{3+} - \text{Ho}^{3+}$ activator system [2]. At times shorter than \bar{T}_d и T_{a3} , kinetics (42) is well described by expression (30). When $2\tau_0 \leq t \ll \bar{T}_d$, T_{a3} , there exists the exponential interval of the kinetics with the quenching rate \bar{W}_1 . For \bar{T}_d , $T_{a3} \ll t \ll T_{a2}$, kinetics (42) has the form

$$n_2^{(2)}(t) = n_0 \exp(-\bar{W}_{1k} t - \Delta), \quad (45)$$

where

$$\bar{W}_{1k} = \bar{T}_d^{-1} + \frac{N_d}{N_a} \bar{W}_1 W_{32} (\bar{W}_2' - \bar{W}_1) \bar{T}_d T_{a3} n_0; \quad (46)$$

$$\begin{aligned} \Delta \approx & \bar{W}_1 \frac{N_d}{N_a} [\bar{W}_3' - \bar{W}_1 - W_{32} (\bar{W}_2' - \bar{W}_1) \\ & \times (\bar{T}_d + T_{a3})] \bar{T}_d T_{a3} n_0. \end{aligned} \quad (47)$$

The physical meaning of expressions describing the donor kinetics in the second approximation is as follows. The difference of the decay rate \bar{W}_{1k} of donor luminescence from the decay rate \bar{T}_d^{-1} obtained in the first approximation is explained by a change in the quenching rate of donors by acceptors due to accumulation of acceptors in the long-lived 5I_7 state. By the beginning of the donor kinetics stage determined by the inequalities \bar{T}_d , $T_{a3} \ll t \ll T_{a2}$, a greater part of donor excitations have been already decayed so that the relation between the concentrations of acceptors in the ground 5I_8 state and acceptors in the long-lived 5I_7 state no longer changes. As a result, the remaining (small) part of excited donors are quenched at the rate depending only on the concentration ratio of acceptors in the 5I_7 and 5I_8 states and also on the ratio of rates of energy transfer from the donor to the acceptor in the 5I_7 state and from the donor to the unexcited acceptor. It is this process that is described by expression (46). In particular, if the effective rate of energy

transfer from the donor to the acceptor in the 5I_7 state is exactly equal to the rate of energy transfer from the donor to the unexcited acceptor (i.e. $\bar{W}'_2 = \bar{W}_1$), no change in the luminescence decay rate of donors will be observed in the final part of the decay curve. Therefore, it follows from (46) that a change in the luminescence decay rate of donors at the stage \bar{T}_d , $T_{a3} \ll t \ll T_{a2}$ compared to the stage $2\tau_0 \leq t \ll \bar{T}_d$, T_{a3} gives information on the ratio of sensitisation rates at the first and second stages of sensitisation of the ${}^5F_5 \rightarrow {}^5I_8$ transition in Ho^{3+} ions. The parameter Δ determined by relation (47) has the physical meaning of a part of donor excitations lost by the time of establishment of the stationary relation between the acceptor concentrations in the ground state and long-lived 5I_7 state. This parameter depends, in particular, on the part of donor excitations lost due to the successive sensitisation of luminescence at the 5S_2 , ${}^5F_4 \rightarrow {}^5I_8$ transition in acceptors. This explains the dependence of Δ on \bar{W}'_3 in (47).

Thus, if at the decay stage \bar{T}_d , $T_{a3} \ll t \ll T_{a2}$ the luminescence decay of donors proceeds with the rate differing from the decay rate at the stage $2\tau_0 \leq t \ll \bar{T}_d$, T_{a3} , the luminescence kinetics of donors provides information on the parameters of donor–acceptor energy transfer at the second stages of step sensitisation of 5S_2 , ${}^5F_4 \rightarrow {}^5I_8$ and ${}^5F_5 \rightarrow {}^5I_8$ transitions. This is the main theoretical result of paper [2].

It follows from relations (46) and (47) that the effective rates \bar{W}'_2 and \bar{W}'_3 are expressed in terms of the parameters \bar{W}_{lk} and Δ as

$$\bar{W}'_2 = \bar{W}_1 + \frac{N_a}{N_d} \frac{\bar{W}_{lk} - \bar{T}_d^{-1}}{\bar{W}_1 W_{32} \bar{T}_d T_{a3} n_0}, \quad (48)$$

$$\begin{aligned} \bar{W}'_3 = & \bar{W}_1 + W_{32}(\bar{W}'_2 - \bar{W}_1)(\bar{T}_d + T_{a3}) \\ & + \frac{\Delta}{\bar{W}_1 \bar{T}_d T_{a3} n_0} \frac{N_a}{N_d}. \end{aligned} \quad (49)$$

In this case, \bar{W}_1 should be determined at the initial stage of the donor kinetics ($t \leq \bar{T}_d$, T_{a3}), while n_0 can be found from measurements of the geometrical parameters of the excitation region and optical losses of exciting radiation in a sample under study.

The rate \bar{W}_{ad5} of inverse energy transfer can be determined from the luminescence decay kinetics of acceptors at the 5S_2 , ${}^5F_4 \rightarrow {}^5I_8$ transition in Ho^{3+} ions observed upon direct optical excitation of the 5S_2 , 5F_4 states of acceptors and also, as shown in [2], by approximating the kinetics of sensitised luminescence at the ${}^5I_6 \rightarrow {}^5I_8$ transition in Ho^{3+} ions by the expression

$$\rho_3^{(2)}(t) = \int_0^t G_3(\tau) \exp\left(-\frac{\tau - t}{T_{a3}}\right) d\tau, \quad (50)$$

where

$$G_3(t) = W_{43} \rho_4^{(1)}(t) + \frac{N_d}{N_a} F_1^{(1)}(t) n_2^{(2)}(t) \times$$

$$\times \left[1 - \rho_2^{(1)}(t) - \rho_3^{(1)}(t) \right] - \frac{N_d}{N_a} \frac{F_3^{(1)}(t) n_2^{(2)}(t) \rho_3^{(1)}(t)}{1 + \bar{W}_{ad5} T_{a5}}, \quad (51)$$

which was obtained for this kinetics in the second approximation for the model under study [2].

The value of \bar{W}_3 is found from the determined values of \bar{W}_{ad5} and \bar{W}'_3 in (44). Then, by using \bar{W}_3 and \bar{W}_{ad5} from (40) and (24), the microparameters C_{da3} and C_{ad5} are determined which characterise the direct and inverse energy transfer at the second stage of the step sensitisation of the 5S_2 , ${}^5F_4 \rightarrow {}^5I_8$ transition in Ho^{3+} ions.

A very small intracentre decay time of the 5F_5 state of Ho^{3+} ions ($T_{a4} \sim 1 \mu\text{s}$) and a weak influence of step sensitisation on the quenching of the intermediate 5I_7 state [3, 4] prevent the experimental measurement of \bar{W}_{ad4} by one of the methods proposed for determining \bar{W}_{ad5} .

Thus, the second approximation for the model under study allows us to find all the quantitative parameters of the second stage of sensitisation of the 5S_2 , ${}^5F_4 \rightarrow {}^5I_8$ transition in Ho^{3+} ions. The parameters of the second stage of sensitisation can be found from kinetics (42) if the initial excitation level n_0 of donors satisfies the condition [2]

$$\frac{\bar{W}_1}{T_d^{-1} + \bar{W}_1} \frac{N_d}{N_a} n_0 \sim 10^{-1} - 1. \quad (52)$$

In [2], the expressions were obtained for kinetics of sensitised luminescence at the rest of the transitions in Ho^{3+} ions, which correspond to the second approximation for the model under study. These kinetics are not presented here because they only slightly differ from (36)–(38) and their analysis does not give any new information on energy transfer and relaxation in the $\text{Yb}^{3+} - \text{Ho}^{3+}$ activator system.

3. Setup for studying luminescence kinetics in $\text{Yb}^{3+} : \text{Ho}^{3+} : \text{GGG}$ crystals and samples

Figure 2 shows the scheme of the experimental setup for studying spectral and kinetic parameters of anti-Stokes luminescence in $\text{Yb}^{3+} : \text{Ho}^{3+} : \text{GGG}$ crystals. The Yb^{3+} ions were excited by a 970.5-nm injection diode laser or a 1.064- μm Q-switched Nd : YAG laser. The Nd : YAG laser

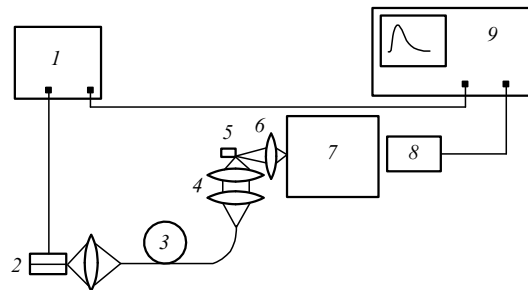


Figure 2. Experimental setup for studying the luminescence kinetics in $\text{Yb}^{3+} : \text{Ho}^{3+} : \text{GGG}$ crystals: (1) unit for formation of pump current pulses of a diode laser and clock pulses; (2) 970.5-nm diode laser or a Nd : YAG laser; (3) optical fibre; (4, 6) focusing optics; (5) $\text{Yb}^{3+} : \text{Ho}^{3+} : \text{GGG}$ crystal sample; (7) MDR-4 monochromator; (8) optical detector (FEU-100, FD-10G or InSb photodiode); (9) TDS 5104 Tektronix digital oscilloscope.

emitted 100-ns pulses. The pulsed operation of the injection laser was provided by using 50- μ s rectangular pump current pulses with a period of 30 ms. The injection laser emitted 1.0-W pulses. The radiation from the diode laser was coupled into a multimode optical fibre with a core of diameter ~ 300 μ m and the numerical aperture $NA = 0.2$. The output radiation from the end of the optical fibre was focused on crystal samples by two lenses.

The luminescence of crystals was collected with a wide-aperture objective in the direction perpendicular to the exciting beam and focused on the entrance slit of an MDR-4 monochromator. The anti-Stokes luminescence of Ho^{3+} ions at 538 or 665 nm was detected with a FEU-100 photomultiplier. The luminescence kinetics of Yb^{3+} and Ho^{3+} ions in the range 0.97–1.21 μ m was detected with an FD-10G photodiode. The luminescence of Ho^{3+} ions in the region of 2 μ m was detected with an InSb photodiode cooled by liquid nitrogen. In the latter case, luminescence was selected with a 2-mm thick germanium plate filter instead of the monochromator. The time constant of each of these optical detectors did not exceed 1 μ s.

The output signals of optical detectors were recorded with a TDS-5104 Tektronix digital oscilloscope. The luminescence kinetics were recorded by averaging over $10^2 - 10^4$ realisations with the time resolution no worse than 2 μ s per count, which considerably improved the signal-to-noise ratio in the detection channel. The oscilloscope was triggered by the leading edge of the exciting optical pulse. The luminescence kinetics were processed by using the ORIGIN 6.0 and Mathcad 2001 Professional programs.

The two $\text{Yb}^{3+} : \text{Ho}^{3+} : \text{GGG}$ crystals under study were grown by the Czochralski method. The atomic concentration of Yb^{3+} and Ho^{3+} in the first crystal was 10 % and 0.1 %, respectively, and in the second crystal – 20 % and 0.3 %. To avoid the reabsorption of luminescence of Yb^{3+} ions, which distorts the kinetics of donors, we studied the luminescence kinetics by using thin plane-parallel crystal plates of thickness 0.1 mm.

In experiments requiring the measurement of the excitation level of Yb^{3+} ions, we estimated the energy E_{abs} of the exciting optical pulse absorbed in a sample and measured the radius R of the optical-beam waist in the sample. The level n_0 of initial excitation of Yb^{3+} ions was determined from the expression

$$n_0 = \frac{P\tau_{\text{imp}}\lambda\{1 - \exp[-\sigma_d(\lambda)N_d l]\}}{\pi R^2 h c N_d}, \quad (53)$$

where l is the sample thickness; h is Planck's constant; c is the speed of light; $\lambda = 970.5$ nm; P is the output cw power of the injection laser; τ_{imp} is the exciting pulse duration; and $\sigma_d(\lambda)$ is the absorption cross section of Yb^{3+} ions at the wavelength λ . The radius R was measured in the focus of the exciting beam by scanning the beam over its cross section with the help of a single-mode fibre with a core of radius 5 μ m, which was fixed on a XYZ stage with a micron drive. The value of R was measured as the half-width at half maximum of the dependence of the radiation intensity at the output of the single-mode optical fibre on the fibre displacement over the beam cross section.

4. Experimental study of donor–donor and donor–acceptor energy transfer in $\text{Yb}^{3+} : \text{Ho}^{3+} : \text{GGG}$ crystals

4.1 Study of the parameters of the first sensitisation stage of Ho^{3+} ions

Figure 3 shows the luminescence kinetics of donors obtained upon weak excitation of samples at 300 K by pulses from the Nd : YAG laser. The donor kinetics in sample 1 is typical for the migration-accelerated quenching regime with the initial static-decay region and exponential decay at the later stage. By approximating this kinetics by dependence (30), we determined the parameters $C_{\text{da}1}$ and m and also τ_0 . The best fit of the experimental kinetics by dependence (30) was obtained for the dipole–dipole mechanism ($m = 6$) of donor–acceptor energy transfer for $C_{\text{da}1} = 9.9 \times 10^{-39}$ $\text{cm}^6 \text{s}^{-1}$ and $\tau_0 = 22$ μ s. Note that the initial static-decay region is not observed in the donor kinetics for sample 2 [curve (2) in Fig. 3]. This is explained by the shortening of the static-decay stage due to the increase in the migration rate with increasing the donor concentration. The decay time \bar{T}_d of donor luminescence measured at 300 K at the stationary stage of the decay kinetics is 388 μ s for sample 1 and 66 μ s for sample 2. Taking into account that $T_d = 1.06$ ms at 300 K, we obtain from (31) that $\bar{W}_1 = 1.1 \times 10^3 \text{s}^{-1}$ for sample 1 and $1.4 \times 10^4 \text{s}^{-1}$ for sample 2. The activator concentration and the obtained values of \bar{W}_1 were substituted together with (33) into (32). The obtained equations for $C_{\text{da}1}$ and C_{dd} were solved numerically by using the Mathcad 2000 Professional packet (the Given and Find operators).

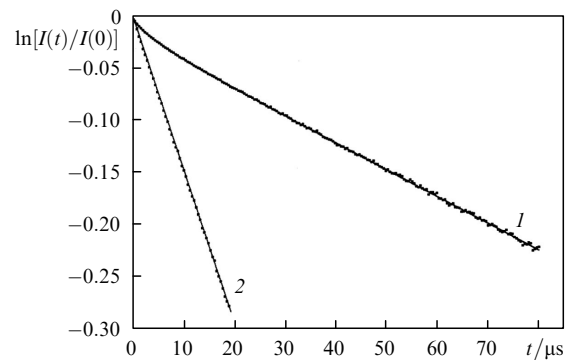


Figure 3. Decay kinetics of donor (Yb^{3+} ions) luminescence in $\text{Yb}^{3+} : \text{Ho}^{3+} : \text{GGG}$ crystals at 300 K observed upon excitation of Yb^{3+} ions by a pulse from a Nd : YAG laser [points are the experimental kinetics, the solid curves are theoretical dependences (30)] for the first (1) and second (2) samples.

The solution of this system of equations for $C_{\text{da}1} = 11 \times 10^{-39}$ $\text{cm}^6 \text{s}^{-1}$ and $C_{\text{dd}} = 3.5 \times 10^{-67}$ $\text{cm}^{10} \text{s}^{-1}$ exists only for $s = 10$ (the quadrupole–quadrupole mechanism of donor–donor energy transfer). Note that $C_{\text{da}1} = 11 \times 10^{-39}$ $\text{cm}^6 \text{s}^{-1}$ found from the solution of the system of equations (32) well coincides with $C_{\text{da}1} = 9.9 \times 10^{-39}$ $\text{cm}^6 \text{s}^{-1}$ obtained by approximating the donor kinetics by expression (30).

The donor kinetics at 77 K were exponential with $\bar{T}_d = 240$ and 39 μ s for samples 1 and 2, respectively. $T_d = 864$ μ s at 77 K, so that $\bar{W}_1 = 2.9 \times 10^3$ and

$2.5 \times 10^4 \text{ s}^{-1}$ for samples 1 and 2, respectively. The micro-parameters C_{dal} and C_{dd} determined in the same way as at temperature 300 K were $8.8 \times 10^{-39} \text{ cm}^6 \text{ s}^{-1}$ and $1.8 \times 10^{-66} \text{ cm}^{10} \text{ s}^{-1}$, respectively.

Note that the obtained data are consistent with theoretical and experimental results reported in paper [9] where it was shown that the microparameter of donor–acceptor energy transfer weakly depends on temperature when energy transfer is nonresonance and is accompanied by the creation of phonons. This takes place in the case of donor–acceptor energy transfer at the first sensitisation stage in the $\text{Yb}^{3+} - \text{Ho}^{3+}$ activator system (Fig. 1). A considerable increase in C_{dd} at 77 K compared to 300 K explains the exponential kinetics of donors at 77 K. In addition, this increase in C_{dd} is in qualitative agreement with the results reported in paper [16], where it was found that the migration rate for Yb^{3+} ions in the garnet lattice achieved a maximum at temperature close to 77 K and was explained by the equality of the homogeneous and inhomogeneous linewidths of Yb^{3+} ions at this temperature.

To verify the validity of the hopping approximation for describing the sensitisation of Ho^{3+} ions in $\text{Yb}^{3+} : \text{Ho}^{3+} : \text{GGG}$ crystals, it is necessary to check the fulfilment of the criterion for hopping approximation for the obtained values of m , s , C_{dd} , and C_{dal} . This criterion has the form [12]:

$$N_{\text{d}} > N_{\text{dc}} = \left(\frac{C_{\text{dal}}}{\gamma C_{\text{dd}}} \right)^{3/(s-m)}, \quad (54)$$

where

$$\gamma = 6 \left[\frac{2\pi}{3} \Gamma \left(1 - \frac{3}{s} \right) \right]^{s/3} \left[s \Gamma \left(\frac{s}{3} \right) \right]^{-1};$$

and $\Gamma(\xi)$ is the Euler gamma function.

It follows from (54) that at 300 K the hopping migration mechanism takes place when $N_{\text{d}} > N_{\text{dc}} = 0.6 \times 10^{21} \text{ cm}^{-3}$ (the atomic concentration $N_{\text{dc}} = 4.7\%$), and at 77 K – when $N_{\text{d}} > N_{\text{dc}} = 1.5 \times 10^{20} \text{ cm}^{-3}$ ($N_{\text{dc}} = 1.2\%$). Thus, the validity of the hopping mechanism for samples 1 and 2 is justified.

The obtained results also allow us to estimate the quantum yield of the first sensitisation stage of transitions in Ho^{3+} ions determined by the expression [7, 12]

$$\eta = 1 - \frac{\bar{T}_{\text{d}}}{T_{\text{d}}}. \quad (55)$$

We obtain from (55) that the quantum yield η at 300 K is 0.63 and 0.94 for samples 1 and 2, respectively. At temperature 77 K, $\eta = 0.72$ and 0.96 for samples 1 and 2, respectively. These values of η suggest that the crystals under study are promising for obtaining lasing at the ${}^5\text{I}_6 \rightarrow {}^5\text{I}_8$, ${}^5\text{I}_6 \rightarrow {}^5\text{I}_7$, and ${}^5\text{I}_7 \rightarrow {}^5\text{I}_8$ transitions in Ho^{3+} ions sensitised due to single-stage energy transfer from excited Yb^{3+} ions.

4.2 Study of the parameters of the second sensitisation stage of Ho^{3+} ions

The Yb^{3+} ions were excited by the injection diode laser. Figure 4 demonstrates the luminescence kinetics of Yb^{3+} ions observed at different excitation levels of the donor subsystem in sample 2. The luminescence kinetics of donors

are coincident at the initial stage. Thus, the decay rate of donor luminescence at the initial stage is independent of the initial excitation level of the donor subsystem and is numerically equal to the stationary decay rate of donor luminescence measured in section 4.1. This is clear because the fraction of excited acceptors at the initial stage is negligible. On the contrary, the decay rate of donor luminescence at the end stage of the kinetics substantially depends on the initial excitation level of the donor subsystem [see (46)], this dependence being stronger at lower decay rates. From the point of view of kinetics (42), this indicates that the rate of energy transfer to the unexcited Ho^{3+} ion exceeds the effective rate of energy transfer to the Ho^{3+} ion in the ${}^5\text{I}_7$ state.

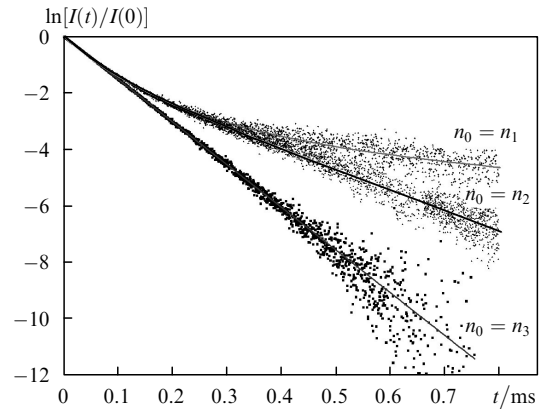


Figure 4. Decay kinetics of donor (Yb^{3+} ions) luminescence in $\text{Yb}^{3+} : \text{Ho}^{3+} : \text{GGG}$ crystals (sample 2) at different donor excitation levels n_0 (300 K, $n_1 > n_2 > n_3$).

Figure 4 illustrates qualitatively the influence of the accumulation of acceptors in a long-lived state on the kinetics of donors. Figure 5 shows the kinetics of donors for sample 1 demonstrating a rather small deviation of the final decay rate from its initial value, which allows us to analyse it quantitatively by using expressions (42)–(49). This kinetics was approximated by expression (42) in two stages. First the value of \bar{W}'_2 was determined from the luminescence quenching rates at the initial (\bar{W}_1) and final (\bar{W}_{1k}) exponential stages of the kinetics by using (48). Then, the value of \bar{W}'_2 was fixed and the value of \bar{W}'_3 in (42) and (43) was varied to obtain the best fit of the experimental kinetics by expression (42). The approximation of the donor kinetics by dependence (42) is also presented in Fig. 5. One can see that expression (42) well describes the experimental data.

The approximation gave $\bar{W}'_3 = 0.8 \times 10^3 \text{ s}^{-1}$ for sample 1 at 300 K. Similarly, analysis of the donor kinetics for sample 2 at 77 K gave $\bar{W}'_3 = 1.5 \times 10^4 \text{ s}^{-1}$.

We determined the rate \bar{W}_{ad5} of inverse energy transfer from the Ho^{3+} ion in the excited ${}^5\text{S}_2$, ${}^5\text{F}_4$ state to the unexcited Yb^{3+} ion in sample 1 by approximating the kinetics of sensitised luminescence at the ${}^5\text{I}_6 \rightarrow {}^5\text{I}_8$ transition in Ho^{3+} ions by dependence (50), as described in section 2. The result of the approximation is presented in Fig. 6. One can see that the kinetics calculated in the second approximation by (50) describes the kinetics of sensitised luminescence at the ${}^5\text{I}_6 \rightarrow {}^5\text{I}_8$ transition in Ho^{3+} ions much better than the kinetics calculated in the first

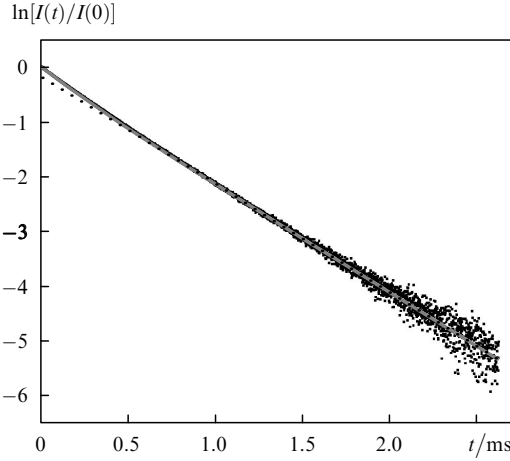


Figure 5. Decay kinetics of donor (Yb^{3+} ions) luminescence in $\text{Yb}^{3+} : \text{Ho}^{3+} : \text{GGG}$ crystals (sample 1) at the initial donor excitation level $n_0 = 1.6\%$ at 300 K; points are the experimental kinetics; the dashed curve is the exponential asymptotics of the final kinetic stage; the grey curve is approximating dependence (42).

approximation (35). The rate of inverse energy transfer determined in this way is $\bar{W}_{\text{ad5}} = 7.5 \times 10^4 \text{ s}^{-1}$ at 300 K and $4.8 \times 10^4 \text{ s}^{-1}$ at 77 K. By using (24), (29), (40), and (44), we obtain $C_{\text{ad5}} = 4.4 \times 10^{-40} \text{ cm}^6 \text{ s}^{-1}$ and $C_{\text{da3}} = 2.1 \times 10^{-38} \text{ cm}^6 \text{ s}^{-1}$ at 300 K and $C_{\text{ad5}} = 1.4 \times 10^{-40} \text{ cm}^6 \text{ s}^{-1}$ and $C_{\text{da3}} = 2.4 \times 10^{-38} \text{ cm}^6 \text{ s}^{-1}$ at 77 K.

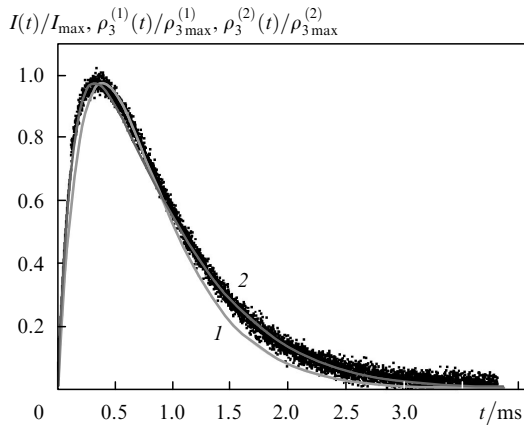


Figure 6. Kinetics of sensitised luminescence at the ${}^5\text{I}_6 \rightarrow {}^5\text{I}_8$ transition in Ho^{3+} ions (sample 1, $n_0 = 1.6\%$, 300 K) calculated (1) in the first approximation (by neglecting inverse energy transfer from the Ho^{3+} ion in the ${}^5\text{S}_2, {}^5\text{F}_4$ state to the unexcited Yb^{3+} ion and accumulation of long-lived acceptors) and (2) in the second approximation (taking into account inverse energy transfer from the Ho^{3+} ion in the ${}^5\text{S}_2, {}^5\text{F}_4$ state to the unexcited Yb^{3+} ion and accumulation of long-lived acceptors); points are the experimental kinetics.

It follows from the data that the difference between the microparameters C_{da3} of the second sensitisation stage at 77 and 300 K is small (as in the case of the first stage). On the contrary, the microparameters of inverse energy transfer differ considerably. This is explained by the fact that inverse energy transfer from the ${}^5\text{S}_2, {}^5\text{F}_4$ level of Ho^{3+} ions to the unexcited Yb^{3+} ion is characterised by the energy deficiency of the order of 200 cm^{-1} , which should be covered by

absorption of one or several phonons. This means that inverse energy transfer is activated with increasing temperature. The direct energy transfer at the second stage of successive sensitisation of the transition under study is accompanied by the creation of phonons and, therefore, weakly depends on temperature.

Similar considerations about the nature of energy transfer at the second stage of successive sensitisation in the $\text{Yb}^{3+} - \text{Ho}^{3+}$ activator system were presented in papers [8, 10]. The experimental results obtained in our paper confirm them.

Figure 7 demonstrates the experimental kinetics of luminescence at transitions of Ho^{3+} ions sensitised by energy transfer approximated by theoretical dependences (36)–(38). Good agreement between the theoretical and experimental dependences confirms the correctness of the scheme of sensitisation and energy relaxation in $\text{Yb}^{3+} : \text{Ho}^{3+} : \text{GGG}$ crystals proposed in section 2.

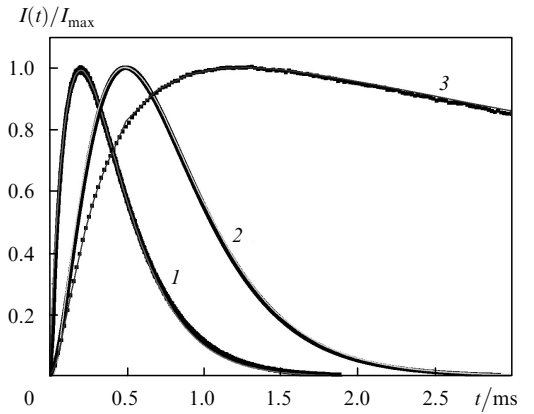


Figure 7. Kinetics of sensitised luminescence at the transitions of Ho^{3+} ions (sample 1, 300 K) at (1) the ${}^5\text{S}_2, {}^5\text{F}_4 \rightarrow {}^5\text{I}_8$ transition [points are the experimental kinetics, the solid curve is dependence (38)], (2) the ${}^5\text{F}_5 \rightarrow {}^5\text{I}_8$ transition [points are the experimental kinetics, the solid curve is dependence (37)], and (3) the ${}^5\text{I}_7 \rightarrow {}^5\text{I}_8$ transition [points are the experimental kinetics, the solid curve is dependence (36)].

Figure 8 presents the dependences of \bar{W}'_3 on the concentration of Yb^{3+} calculated by (24), (33), (40), and (44) for the measured parameters of direct and inverse energy transfer. As the concentration of donors is increased, both the migration rate and the rate of inverse energy transfer from the ${}^5\text{S}_2, {}^5\text{F}_4$ level increase, which explains the presence of a maximum of dependences in Fig. 8. Note that the concentration N_{dmax} of Yb^{3+} ions corresponding to the maximum $\bar{W}'_{3\text{max}}$ of the dependence of \bar{W}'_3 on the concentration of Yb^{3+} ions is optimal for obtaining lasing at the sensitised ${}^5\text{S}_2, {}^5\text{F}_4 \rightarrow {}^5\text{I}_8$ transition in Ho^{3+} ions.

It should be emphasised that the atomic concentration N_{dmax} is the same for all concentrations of Ho^{3+} ions and is 41% at 300 K and 27% at 77 K. One can see from Fig. 8 that the maximum rate $\bar{W}'_{3\text{max}} = 1.7 \times 10^3 \text{ s}^{-1}$ of energy transfer at 300 K is lower than the relaxation rate $T_{\text{a3}}^{-1} = 2.6 \times 10^3 \text{ s}^{-1}$ of the intermediate ${}^5\text{I}_6$ state. At temperature 77 K, the maximum rate $\bar{W}'_{3\text{max}} = 5.1 \times 10^3 \text{ s}^{-1}$ of energy transfer considerably exceeds the relaxation rate $T_{\text{a3}}^{-1} = 2.4 \times 10^3 \text{ s}^{-1}$ of this intermediate state. As follows from (40) and (41), the rate \bar{W}'_3 is directly proportional to the concentration of Ho^{3+} ions.

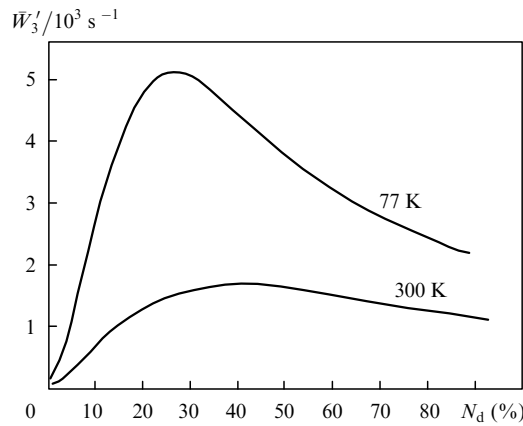


Figure 8. Dependences of the effective rate of energy transfer at the second sensitisation stage of the ${}^5S_2, {}^5F_4 \rightarrow {}^5I_8$ transition in Ho^{3+} ions on the atomic concentration of donors (0.1% of Ho^{3+}) at different temperatures.

The dependences in Fig. 8 are plotted for the atomic concentration of Ho^{3+} ions equal to 0.1%, so that for $N_d \approx N_{d\max}$ and the concentration of Ho^{3+} ions of about 0.3%–0.5%, the effective rate \bar{W}_3' of energy transfer will considerably exceed the relaxation rate of the intermediate 5I_6 level both at 77 and 300 K. The atomic concentrations of Ho^{3+} exceeding 0.5% are unfavourable for obtaining lasing at the ${}^5S_2, {}^5F_4 \rightarrow {}^5I_8$ transition in Ho^{3+} ions because of the cross-relaxation quenching of the ${}^5S_2, {}^5F_4$ states [6, 8, 10]. Thus, the obtained experimental data suggest that $\text{Yb}^{3+} : \text{Ho}^{3+} : \text{GGG}$ crystals can be promising for obtaining lasing in the green spectral region at the sensitised ${}^5S_2, {}^5F_4 \rightarrow {}^5I_8$ transition in Ho^{3+} ions. Note that the rate W_{32} of intracentre relaxation from the intermediate 5I_6 state to the long-lived 5I_7 state for crystals under study is $1.3 \times 10^3 \text{ s}^{-1}$. Therefore, to obtain lasing at the ${}^5S_2, {}^5F_4 \rightarrow {}^5I_8$ transition in Ho^{3+} ions, pulsed pumping of the ${}^2F_{7/2} \rightarrow {}^2F_{5/2}$ transition in Yb^{3+} ions is desirable. In this case, the pump pulse duration should not exceed $W_{32}^{-1} \sim 0.7\text{--}0.8$ ms and the pulse repetition period should be shorter than 30 ms to avoid the accumulation of Ho^{3+} ions in the long-lived 5I_7 state ($T_{a2} \sim 8\text{--}9$ ms). It is advantageous to use the same pump regime to obtain lasing at the sensitised ${}^5I_6 \rightarrow {}^5I_8$ and ${}^5I_6 \rightarrow {}^5I_7$ transitions in Ho^{3+} ions.

The step sensitisation of the ${}^5S_2, {}^5F_4 \rightarrow {}^5I_8$ transition in Ho^{3+} ions is unfavourable for obtaining lasing at the ${}^5I_7 \rightarrow {}^5I_8$ transition in these ions. To obtain lasing at this transition, it is expedient to use $\text{Yb}^{3+} : \text{Ho}^{3+} : \text{GGG}$ crystals with the atomic concentration of Ho^{3+} of 2%–5% providing the efficient cross relaxation quenching of the ${}^5S_2, {}^5F_4$ state [6, 8, 10]. The calculation of the dependence of \bar{W}_1 on N_d showed that, to obtain lasing at this transition, the concentration of Yb^{3+} should exceed 50% at 300 K and 30% at 77 K. Note also that the step sensitisation of the ${}^5F_5 \rightarrow {}^5I_8$ transition in Ho^{3+} ions in the crystals under study is weak and does not cause any considerable quenching of the intermediate 5I_7 state of Ho^{3+} ions.

5. Conclusions

We have studied experimentally the luminescence kinetics of donors (Yb^{3+} ions) and acceptors (Ho^{3+} ions) in $\text{Yb}^{3+} : \text{Ho}^{3+} : \text{GGG}$ crystals upon excitation of Yb^{3+} ions by short laser pulses. The kinetics were analysed by using

the model of step hopping sensitisation of luminescence [2]. Good agreement between the experimental data and theoretical calculations has been obtained. The qualitative and quantitative analysis of luminescence kinetics observed in $\text{Yb}^{3+} : \text{Ho}^{3+} : \text{GGG}$ crystals has shown that:

(i) The donor–acceptor energy transfer in $\text{Yb}^{3+} : \text{Ho}^{3+} : \text{GGG}$ crystals is described by the dipole–dipole mechanism.

(ii) The donor–donor energy transfer in $\text{Yb}^{3+} : \text{Ho}^{3+} : \text{GGG}$ crystals is described by the quadrupole–quadrupole mechanism with the microparameter $C_{dd} = 3.5 \times 10^{-67} \text{ cm}^{10} \text{ s}^{-1}$ at 300 K and $1.8 \times 10^{-66} \text{ s}^{-1}$ at 77 K.

(iii) Energy transfer from the excited Yb^{3+} ion to the unexcited Ho^{3+} ion is nonresonant and irreversible and is accompanied by the transition of the Ho^{3+} ion to the 5I_6 state. The microparameter of this energy transfer process is $C_{da1} = 11 \times 10^{-39} \text{ cm}^6 \text{ s}^{-1}$ at 300 K and $8.8 \times 10^{-39} \text{ cm}^6 \text{ s}^{-1}$ at 77 K.

(iv) Energy transfer from the excited Yb^{3+} ion to the excited Ho^{3+} ion in the 5I_6 state is reversible and is accompanied by the transition of the Ho^{3+} ion to the ${}^5S_2, {}^5F_4$ state. The microparameter of energy transfer is $C_{da3} = 2.1 \times 10^{-38} \text{ cm}^6 \text{ s}^{-1}$ at 300 K and $2.4 \times 10^{-38} \text{ cm}^6 \text{ s}^{-1}$ at 77 K. The microparameter C_{ad5} of inverse energy transfer from the Ho^{3+} ion in the ${}^5S_2, {}^5F_4$ state to the unexcited Yb^{3+} ion is $4.4 \times 10^{-40} \text{ cm}^6 \text{ s}^{-1}$ at 300 K and $1.4 \times 10^{-40} \text{ cm}^6 \text{ s}^{-1}$ at 77 K.

(v) The specific features of the donor and acceptor kinetics caused by the accumulation of long-lived acceptors and the influence of two-step sensitisation predicted in [2] were experimentally observed in $\text{Yb}^{3+} : \text{Ho}^{3+} : \text{GGG}$ crystals. These features were observed already at the excitation level of donors of $\sim 1\%$ when the concentration of donors was two orders of magnitude higher than that of acceptors.

(vi) In the case of optimal concentrations of donors and acceptors in $\text{Yb}^{3+} : \text{Ho}^{3+} : \text{GGG}$ crystals, the effective rate of energy transfer at the second sensitisation stage of the ${}^5S_2, {}^5F_4 \rightarrow {}^5I_8$ transition can exceed the relaxation rate of the intermediate 5I_6 level. This suggests that the $\text{Yb}^{3+} : \text{Ho}^{3+} : \text{GGG}$ crystals are promising for obtaining lasing in the green spectral region at the sensitised ${}^5S_2, {}^5F_4 \rightarrow {}^5I_8$ transition in Ho^{3+} ions pumped into the ${}^2F_{7/2} \rightarrow {}^2F_{5/2}$ absorption band of Yb^{3+} ions. According to the estimate, the optimal atomic concentrations of donors and acceptors for lasing at the sensitised ${}^5S_2, {}^5F_4 \rightarrow {}^5I_8$ transition are 30%–50% for Yb^{3+} and 0.3%–0.5% for Ho^{3+} at 300 K and 20%–35% for Yb^{3+} and 0.3%–0.5% for Ho^{3+} at 77 K. To obtain lasing at the ${}^5S_2, {}^5F_4 \rightarrow {}^5I_8$ transition in Ho^{3+} ions, it is advantageous to use pulsed pumping of Yb^{3+} ions at the ${}^2F_{7/2} \rightarrow {}^2F_{5/2}$ transition. In this case, the pump pulse duration should not exceed 0.7–0.8 ms and the pulse repetition period should be shorter than 30 ms to avoid the accumulation of Ho^{3+} ions in the long-lived 5I_7 state.

(vii) The crystals studied in the paper are promising for obtaining lasing at the ${}^5I_7 \rightarrow {}^5I_8$ transition in Ho^{3+} ions upon pumping into the absorption band of Yb^{3+} ions. The optimal atomic concentrations of donors and acceptors in this case are 50%–60% for Yb^{3+} and 2%–5% for Ho^{3+} at 300 K and 30%–40% for Yb^{3+} and 2%–5% for Ho^{3+} at 77 K.

References

1. Diening A., Kuck S. *J. Appl. Phys.*, **87** (9), 4063 (2000).
2. Belovolov A.M., Belovolov M.I., Dianov E.M., Timoshechkin M.I. Preprint IOFRAN, No. 10 (Moscow, 2006).
3. Rothacher T., Lüthy W., Weber H.P. *Opt. Commun.*, **155**, 68 (1998).
4. Zavaritsev Yu.D., Osiko V.V., Semenov S.G., Studenikin P.A., Umyskov A.F. *Kvantovaya Elektron.*, **20**, 366 (1993) [*Quantum Electron.*, **23**, 312 (1993)].
5. Johnson L.F., Cuggenheim H.J. *Appl. Phys. Lett.*, **19**, 44 (1971).
6. Trash R.J., Jarman R.H., Chai B.N.T., Pham A. *Compact Blue-Green Lasers* (Washington, DC: OSA Techn. Digest Series, 1994) Vol.1, Paper CFA.
7. Walti R., Lüthy W., Weber H.P., Rusanov S.Ya., Yakovlev A.A., Zagumenyi A.I., Shcherbakov I.A., Umyskov A.F. *J. Quantum Spectrosc. Radiat. Transfer*, **54** (4), 671 (1995).
8. Martin I.R., Rodrigues V.D., Lavin V., Rodrigues-Mendoza U.R. *J. Alloys and Compounds*, **227–228**, 345 (1998).
9. Alekseev N.E., Gapontsev V.P., Zhabotinskii M.E., Kravchenko V.B., Rudnitskii Yu.P. *Lazernye fosfatnye stekla* (Laser Phosphate Glasses) (Moscow: Nauka, 1980).
10. Zhang X.X., Hong P., Bass M., Chai B.H.T. *Compact Blue-Green Lasers* (Washington, DC: OSA Techn. Digest Series, 1994) Vol.1, Paper CFA4.
11. Kir'yanov A.V., Aboites V., Belovolov A.M., Timoshechkin M.I., Belovolov M.I., Damzen M.J., Minassian A. *Opt. Express*, **10** (16), 832 (2002).
12. Burshtein A.I. *Usp. Fiz. Nauk*, **143**, 553 (1984).
13. Zusman L.D. *Opt. Spekt.*, **36**, 497 (1974).
14. Zusman L.D. *Zh. Eksp. Teor. Fiz.*, **73**, 662 (1977).
15. Privis Yu.S., Smirnov V.A., Shcherbakov I.A. *Zh. Eksp. Teor. Fiz.*, **87**, 589 (1984).
16. Basiev T.T. *Cand. Diss.* (Moscow: FIAN, 1976) pp 79–94.